

EXACT BYTE-LEVEL PROBABILITIES FROM TOKENIZED LANGUAGE MODELS FOR FIM-TASKS AND MODEL ENSEMBLES

Anonymous authors

Paper under double-blind review

ABSTRACT

Tokenization is associated with many poorly understood shortcomings in language models (LMs), yet remains an important component for long sequence scaling purposes. This work studies how tokenization impacts model performance by analyzing and comparing the stochastic behavior of tokenized models with their byte-level, or token-free, counterparts. We discover that, even when the two models are statistically equivalent, their predictive distributions over the next byte can be substantially different, a phenomenon we term as “tokenization bias”. To fully characterize this phenomenon, we introduce the Byte-Token Representation Lemma, a framework that establishes a mapping between the learned token distribution and its equivalent byte-level distribution. From this result, we develop a next-byte sampling algorithm that eliminates tokenization bias without requiring further training or optimization. In other words, this enables zero-shot conversion of tokenized LMs into statistically equivalent token-free ones. We demonstrate its broad applicability with two use cases: fill-in-the-middle (FIM) tasks and model ensembles. In FIM tasks where input prompts may terminate mid-token, leading to out-of-distribution tokenization, our method mitigates performance degradation and achieves an approximately 18% improvement in FIM coding benchmarks, consistently outperforming the standard token healing fix. For model ensembles where each model employs a distinct vocabulary, our approach enables seamless integration, resulting in improved performance (up to 3.7%) over individual models across various standard baselines in reasoning, knowledge, and coding.

1 INTRODUCTION

Transformers form the backbone of all widely-used state-of-the-art language models (LMs) such as GPTs (Brown et al., 2020), Llama (Touvron et al., 2023), and Mistral (Jiang et al., 2023a). A common pre-processing step in these models is tokenization, a method that shortens the input sequence by mapping multiple bytes, i.e. characters into discrete tokens, i.e. words or subwords, from a fixed vocabulary¹. Efforts to bypass tokenization have shown limited empirical success (Yu et al., 2024; Limisiewicz et al., 2024), suggesting tokenization is critical to the performance of large language models (LLMs). It has been speculated that the reason for the performance gap between tokenized and byte-level models is due to the reduction of input tokens, allowing models to handle longer contexts at less compute (Zouhar et al., 2023; Goldman et al., 2024). Recent work by Rajaraman et al. (2024) provides an additional explanation: Even for unlimited data and compute², tokenized models can achieve better cross-entropy loss than untokenized ones, resulting in superior performance.

To contribute to the understanding of the impact of tokenization, we demonstrate that for any tokenized LM, there exists a statistically equivalent byte-level process. Despite their statistical equivalence in terms of training loss, we find a surprising discrepancy in their predictive behaviors—particularly in next-token and next-byte predictions, where there can be significant differences. We hence introduce the concept of *tokenization bias* to describe the discrepancy between

¹In the context of this study, we use the terms “character” and “byte” interchangeably to refer to an element from a subset of the tokenization vocabulary. This subset is somewhat flexible. Precision is only important in the experiment section where we define the subset to be all utf-8 bytes.

²And assuming the data source can be approximated as a k^{th} order Markov chain.

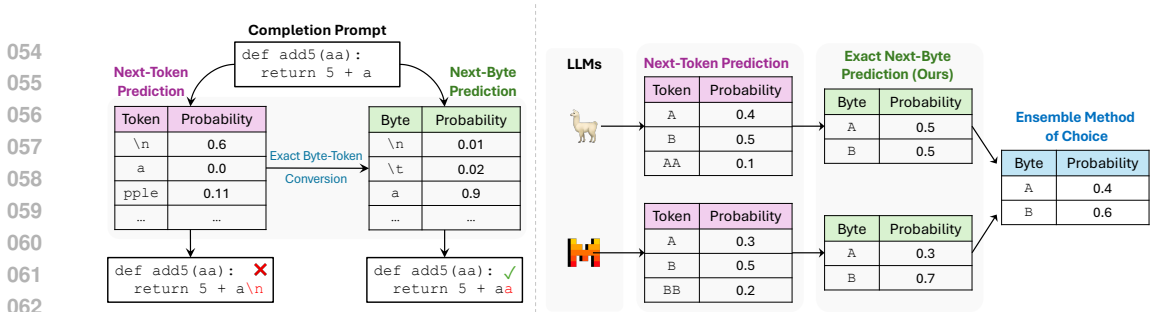


Figure 1: **Left:** Tokenized LMs can experience tokenization bias when prompts end mid-token, as in this code completion example. This means that the correct solution, `a` has zero probability of being chosen. Our method avoids this problem and can predict the correct token while using the same model. **Right:** Our method maps next-token predictions of arbitrary tokenized LMs to statistically equivalent next-byte predictions (see Section 4.1 for details). This enables any model ensemble strategy, such as averaging or mixture of experts.

the predictive distributions of the tokenized model and the byte-level equivalent. Towards *mapping tokenized predictions to byte-level predictions*, we present the Byte-Token Representation Lemma (Section 4.1). The lemma enables both byte-level predictions and an algorithmic correction of tokenization bias in any trained LM without the need for additional training or optimization, allowing us to *sample bias-free next-bytes from any tokenized LM*.

Because our findings show that tokenization introduces an irreducible gap between the token and byte domains by preventing certain token combinations, limiting the model’s ability to sample specific tokens, we investigate this issue in fill-in-the-middle (FIM) tasks. Tokenization bias is particularly harmful in fill-in-the-middle (FIM) tasks when a prompt ends mid token. Tokenized language models struggle to predict the correct completion (Dagan et al., 2024). Our theory predicts this phenomenon precisely, and the failure example shown in Figure 1 (Left) can be reproduced with any open-weight model to date. In our experiments, we demonstrate that our next-byte prediction method outperforms tokenized models with the same cross-entropy by 18%, and even surpasses a specialized fix, token healing (Dagan et al., 2024; Roziere et al., 2023), by 1%.

A byproduct of our byte-level prediction algorithm is that it enables ensembling of arbitrary LMs. Ordinarily, one cannot average the predictions of LMs that do not share a vocabulary. However, by mapping their predictions and conditioning domains to byte-space, one can easily aggregate predictions from multiple models and leverage the benefits of ensembling. Combining multiple models is advantageous because model ensembles are generally more accurate and robust than any individual member (Hastie et al., 2009). We also confirm this experimentally: models that are ensembled using our byte-level predictions outperform individual models in many cases.

In summary, the key contributions of this work are:

1. We convert tokenized LMs into statistically equivalent token-free models, and demonstrate that their predictive distributions differ. We define this discrepancy as tokenization bias.
2. We introduce a method that enables next-byte prediction for any tokenized language model to fully mitigate tokenization bias. This algorithm is applied at inference time and carries an $O(1)$ computational cost in terms of model runs.
3. We present strong empirical evaluations on an FIM benchmark (18% improvement) and model ensemble tasks (up to 3.7% improvement), further demonstrating the effectiveness of our approach.

2 NOTATIONS AND SETUP

2.1 STRING AND BYTE-LEVEL LANGUAGE MODELS

We denote the alphabet set as \mathcal{A} and its element character, or byte, as x . By default and consistent with real-world data, unless otherwise stated, we include the end of string `<EOS>` byte in \mathcal{A} . For any (finite) string s , we denote its substring from location i to j as $x_i^j := x_i x_{i+1} \dots x_j$. We view any byte-level LM as a discrete stochastic process that defines the autoregressive probability $P(x_{n+1} | x_1^n)$ for all n . This defines an infinite (stochastic) sequence $\mathbf{x} = x_1 x_2 \dots$ where $\mathbf{x} \in \mathcal{X}$. With the existence of

108 $\langle \text{EOS} \rangle$, we have $P(x_{n+1}|x_1^n) = 1.0$ for $x_{n+1} = x_n = \langle \text{EOS} \rangle$ and $P(x_{n+1} = \langle \text{EOS} \rangle | x_1^n) \neq 0.0$
 109 for any x_1^n . This means all \mathbf{x} effectively have finite length and the set \mathcal{X} is countably infinite. We
 110 refer to \mathbf{x} as a byte sequence instead of a string, which has a finite length and does not necessarily
 111 end with $\langle \text{EOS} \rangle$.

112 Given x_1^n , the function `prefix(.)` returns all possible prefixes of x_1^n , i.e. $\text{prefix}(x_1^n) =$
 113 $\{x_1^1, x_1^2, x_1^3, \dots, x_1^n\}$. We denote the concatenation operation as `concat(.)`, i.e. $\text{concat}(x_1^{n_1}, y_1^{n_2}) =$
 114 $x_1 \dots x_{n_1} y_1 \dots y_{n_2}$. Furthermore, we define $\mathcal{X}(x_1^n)$ as the set consisting of all infinite sequence \mathbf{x} with
 115 prefix x_1^n , i.e.

$$116 \mathcal{X}(x_1^n) = \{\mathbf{x} | x_1^n \in \text{prefix}(\mathbf{x})\},$$

117 which corresponds to the byte-level probability of obtaining a sequence with prefix x_1^n , or $P(x_1^n)$.

118 2.2 TOKENIZED LANGUAGE MODELS

121 We consider two commonly used tokenization algorithms, namely Byte-Pair Encoding (BPE) (see
 122 Algorithm 2 in Appendix A.4) and Maximum Prefix Encoding (MPE). Tokens are elements within
 123 a vocabulary \mathcal{V} , where $\mathcal{A} \subseteq \mathcal{V}$, an individual token is denoted as $t \in \mathcal{V}$. We also assume $\langle \text{EOS} \rangle$
 124 is not a part of any token but itself. An encoding of length k of a string x_1^n is $t_1^k = \text{encode}(x_1^n)$.
 125 Conversely, a decoding of t_1^k is a string denoted as $x_1^n = \text{decode}(t_1^k)$. Encodings with an unspecified
 126 number of tokens are denoted as \vec{t} and $\vec{t}_{[i:j]}$ are the elements from i to j of \vec{t} . Note that BPE and
 127 MPE are deterministic, i.e. each string s and sequence \mathbf{x} correspond to a unique encoding (lossless
 128 compression). Furthermore, we define $\mathcal{X}(t_1^k)$ as a set consisting of all sequences whose encodings
 129 start with t_1^k , i.e.

$$130 \mathcal{X}(t_1^k) = \{\mathbf{x} | t_1^k = \text{encode}(\mathbf{x})_1^k\},$$

131 which corresponds to the token-level probability $P(t_1^k)$, i.e. the probability of obtaining a sequence
 132 whose encoding starts with t_1^k . We also view any tokenized LM as an autoregressive process that
 133 defines $P(t_{k+1}|t_1^k)$ and refer to an infinite token sequence as $\mathbf{t} = t_1 t_2 \dots$ and $\mathbf{t} \in \mathcal{T}$. Similar as the
 134 byte-level process, with the existence of $\langle \text{EOS} \rangle$, \mathbf{t} is effectively finite and \mathcal{T} is countably infinite.

135 3 LANGUAGE MODELS AND TOKENIZATION BIAS

136 3.1 STATISTICAL EQUIVALENCE BETWEEN DATA GENERATING PROCESSES

137 We begin by establishing the definition of statistical equivalence between two stochastic processes.
 138 Then, we show that byte-level LMs and their induced tokenized LMs are statistically equivalent.

139 **Definition 1.** (Statistical Equivalence) For a countably infinite set \mathcal{X} , the byte-level data generating
 140 processes \mathcal{G}_1 and \mathcal{G}_2 are statistically equivalent if and only if:

$$141 P_{\mathcal{G}_1}(\mathbf{x}) = P_{\mathcal{G}_2}(\mathbf{x}) \text{ for all } \mathbf{x} \in \mathcal{X},$$

142 i.e., the chance of sampling a sequence \mathbf{x} are identical for processes \mathcal{G}_1 and \mathcal{G}_2 , denoted by their
 143 subscripts.

144 We consider the following two stochastic processes:

- 145 • \mathcal{G}_1 : the ground truth byte-level language models $P(x_{n+1}|x_1^n)$.
- 146 • \mathcal{G}_2 : consists of the tokenized model $P(t_{k+1}|t_1^k)$ induced from the process \mathcal{G}_1 and tokeniza-
 147 tion. The process \mathcal{G}_2 generates sequence \mathbf{x} by autoregressively sampling new t_{k+1} and
 148 maps t_{k+1} to its byte-level representation using the `decode(.)` function.

149 Since the mapping defined by the tokenizer for the sequence \mathbf{x} and its encoding $\mathbf{t} = \text{encode}(\mathbf{x})$ is
 150 bijective, we have $P(\mathbf{t}) = P(\mathbf{x})$, leading to two processes being statistically equivalent. This implies
 151 that it is possible to convert any tokenized LM to its statistically equivalent byte-level counterpart.

152 3.2 TOKENIZATION BIAS

153 Despite their statistical equivalence, the generation behavior of tokenized and byte-level LMs can
 154 be significantly different when prompted with the same string. We characterize the tokenization bias
 155 phenomenon that describes this discrepancy between conditioning domains, i.e. bytes versus tokens.

162
163
164
165
166
167
168
169
170
171
172
173
174
175
176
177
178
179
180
181
182
183
184
185
186
187
188
189
190
191
192
193
194
195
196
197
198
199
200
201
202
203
204
205
206
207
208
209
210
211
212
213
214
215

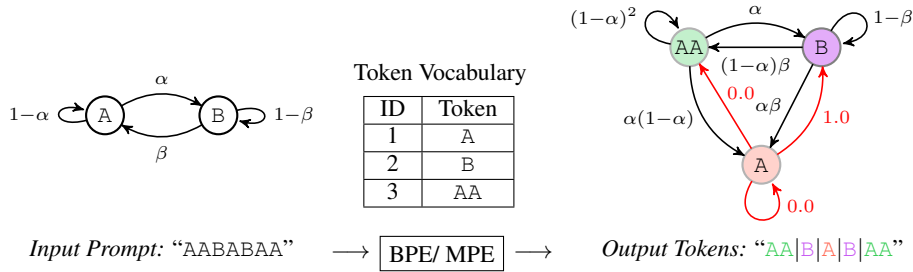


Figure 2: Tokenization bias on a 1st-order Markov chain. Given the context token “A”, the model will never sample the next token as “A”, rather than with probability $1 - \alpha$. In practice, this bias occurs when prompts end with tokens that are part of another token, a common issue in the FIM tasks, leading to incorrect completions by the model.

Definition 2. (Tokenization Bias) Let the input prompt x_1^n have the corresponding encoding $t_1^k = \text{encode}(x_1^n)$. The tokenization bias occurs for this prompt when:

$$P(x_{n+1}|x_1^n) \neq P(x_{n+1}|t_1^k), \tag{1}$$

where $P(x_{n+1}|t_1^k) = \sum_{t \in \mathcal{E}} P(t_{k+1}=t|t_1^k)$ and $\mathcal{E} = \{t \in \mathcal{V} | x_{n+1} = \text{decode}(t)_1\}$, i.e. the set of tokens whose first byte is x_{n+1} .

For example, the probability of the next byte being “c” may be different from the sum of the probabilities of all tokens that start with “c”, which offers a broader perspective compared to the probability of the subsequent token being exactly “c”.

3.2.1 TOKENIZATION BIAS IN MARKOV CHAINS

To systematically study tokenization bias, we employ a simplified autoregressive model, representing the data generating process as a Markov chain. As a result, we can derive a closed-form expression for the induced tokenized model and directly observe the tokenization bias phenomenon.

We consider a 1st order Markov chain with two states {“A”, “B”}, shown in Figure 2 (left) where each string is tokenized with either MPE or BPE, which yields the same result. With the vocabulary $\mathcal{V} = \{“AA”, “A”, “B”\}$, we obtain a new Markov chain whose states and transition matrix are shown in Figure 2 (right). Appendix A.7 provides details on computing the transition matrix. The statistical equivalency between two chains is described in Rajaraman et al. (2024). First, notice that no tokenization bias occurs when conditioning on $t_1 = “AA”$ or $t_1 = “B”$, e.g.

$$P(x_3 = “A” | x_1^2 = “AA”) = P(t_2 = “AA” | t_1 = “AA”) + P(t_2 = “A” | t_1 = “AA”) = 1 - \alpha$$

However, when conditioning on $t_1 = “A”$, tokenization bias emerges, i.e. the probability $P(x_2 = “A” | t_1 = “A”) = 0.0$ is not equal to $P(x_2 = “A” | x_1 = “A”) = 1 - \alpha$, i.e. the token-level Markov chain never samples “A” with any prompt ending with token “A”. The reason is that whenever two consecutive bytes “A” appear together, the tokenizer immediately merges them into a single token “AA”, results in zero probability. Despite being simple, this model portrays the exact phenomenon as the coding example discussed in Figure 1(Left).

Higher-Order Markov Chain. We now show this phenomenon in a more complex, 3rd order Markov chain, but shift from mathematical derivation to an empirical approach to demonstrate its relevance in practice. Furthermore, we leverage this example to illustrate the effectiveness of our byte-token conversion method, to be introduced in Section 4, as a viable bias correction technique. Here, we train a decoder transformer on tokenized data and analyse its next-token probabilities, shown in Figure 3. As we expect, the trained tokenized model exhibits severe bias in its predictions. Nevertheless, when combined with our bias correction technique, we accurately recover the original transition probabilities, demonstrating its potential for generalization to other LMs. We detail the experiment setup in Appendix A.7.

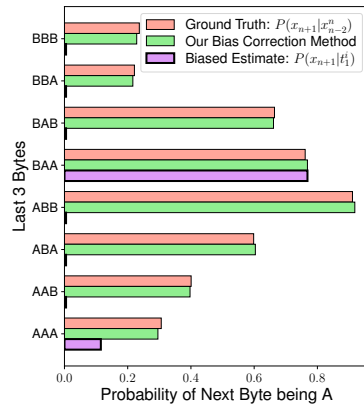


Figure 3: Tokenization bias on a 3rd order Markov chain. Our byte-token conversion (bias correction) method in Section 4 accurately recovers $P(x_{n+1}|x_1^n)$ of the original chain.

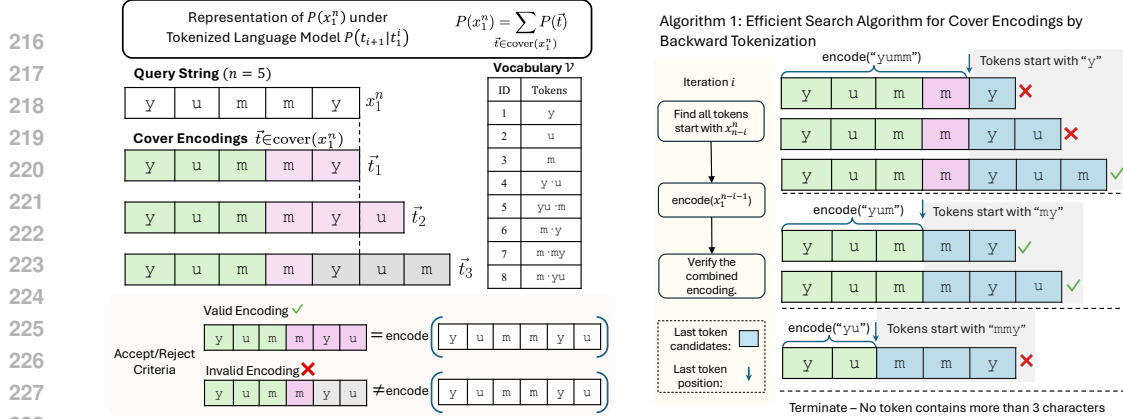


Figure 4: **Left:** Representation of $P(x_1^n)$ using tokenized LM with an example of cover encodings and valid/invalid encoding. **Right:** Illustration of Algorithm 1 for cover encodings search. Green tick and red cross denote valid and invalid encodings respectively (Definition 3). The termination step can be easily implemented despite not shown in the algorithm. We use BPE in this example.

3.2.2 INVALID ENCODINGS

The investigation on the zero probability events observed in our Markov chain example leads us to introduce the definition of invalid encodings, which sets constraints on the probability $P(\vec{t})$ of tokenized LMs.

Definition 3. (Invalid Encodings) An encoding \vec{t} is invalid if $\text{encode}(\text{decode}(\vec{t})) \neq \vec{t}$, else it is valid.

In other words, invalid encodings represent the string with different tokens than the one produced by the tokenizer. For example, assume MPE tokenizer and $\mathcal{V} = \{“c”, “a”, “t”, “at”, “cat”\}$, then $\text{encode}(“catt”) = [“cat”, “t”]$. Encodings $[“c”, “at”, “t”]$ and $[“c”, “a”, “t”, “t”]$ are invalid.

With this definition, Proposition 1 states that no invalid encodings will exist in the token distribution.

Proposition 1. $\mathcal{X}(t_1^k) = \emptyset$ if and only if t_1^k is invalid. As a result, $P(t_1^k) = 0.0$. Furthermore, $P(t_k | t_1^{k-1}) = 0.0$ if t_1^{k-1} is valid, otherwise, it is undefined.

Proof. See Appendix A.4

We note that Proposition 1 indicates the constraints of $P(t_1^k)$ for tokenized LM induced the by byte-level data generating process. For trained LMs, $P(t_k | t_1^{k-1})$ is not zero for invalid t_1^k due to softmax activations. Nevertheless, we observe it to be very low compared to the valid t_1^k , as in Figure 3. Finally, we can truncate these invalid probability to zero without any loss in terms of perplexity score, detailed in Appendix A.6.

4 EXACT BYTE-LEVEL PROBABILITIES

4.1 BYTE-TOKEN REPRESENTATION LEMMA FOR $P(x_1^n)$

To address the tokenization bias, we derive byte-level predictions $P(x_{n+1} | x_1^n)$ from token-level predictions $P(t_{k+1} | t_1^k)$. To this end, we compute $P(x_1^n)$ and begin with the concept of cover encodings of x_1^n . These encodings are valid encodings that “optimally” contain x_1^n , i.e. their last tokens start at locations $i < n$. Results in this section, i.e. Section 4.1, apply for any deterministic tokenizer, not just BPE/ MPE.

Definition 4. (Cover Encodings) Given a prefix x_1^n , an encoding t_1^k is said to be covering x_1^n when all the following conditions satisfied:

1. t_1^k is valid.
2. $x_1^n \in \text{prefix}(\text{decode}(t_1^k))$.
3. $x_i^n \in t_k$ for some $1 \leq i \leq n$, i.e. the last token t_k covers a part of the string x_1^n .

We denote $\text{cover}(x_1^n)$ to be the set of all cover encodings of x_1^n , with examples in Figure 4 (mid-left).

Following the definition of cover encoding, we establish the BTR Lemma that allows us to exactly compute $P(x_1^n)$ using $P(t_{k+1}|t_1^k)$. The idea of the BTR Lemma is that for any sequence \mathbf{x} starting with x_1^n , its encoding $\text{encode}(\mathbf{x})$ must start with one of the encodings in $\text{cover}(x_1^n)$.

Lemma 1. (*Byte-Token Representation Lemma*) For a language model $P(t_{k+1}|t_1^k)$, given a prefix x_1^n , the following statements hold:

1. For any distinct $\vec{t}, \vec{t}' \in \text{cover}(x_1^n)$, we have $\mathcal{X}(\vec{t}) \cap \mathcal{X}(\vec{t}') = \emptyset$.
2. $\mathcal{X}(x_1^n) = \bigcup_{\vec{t} \in \text{cover}(x_1^n)} \mathcal{X}(\vec{t})$.

As a result, $P(x_1^n)$ can be expressed as the marginal probability of all covering tokens of x_1^n

$$P(x_1^n) = \sum_{\vec{t} \in \text{cover}(x_1^n)} P(\vec{t}). \quad (2)$$

Proof. See Appendix A.2.

Remark 1. The BTR Lemma provides a general view of tokenization bias. Consider the cover encoding example in Figure 4 (middle-left). There, given the input string $x_1^5 = \text{"yummy"}$, prompting into the models $\text{encode}(x_1^5) = [\text{"yum"}, \text{"my"}]$ will discard the other two possibilities, resulting in a skew distribution over the next-byte, i.e. tokenization bias.

Some scenarios requires conditioning on special tokens, such as when using control/synthetic tokens (e.g., FIM code-infilling). In such cases, we want to compute the byte-level probability conditioned on specific tokens, i.e. $P(x_{m+1}^n | t_1^k)$ where $x_1^n = \text{decode}(t_1^k)$, or equivalently, $P(x_1^n, t_1^k)$. Corollary 1 provides a closed-form expression for this quantity.

Corollary 1. We can express $P(x_1^n, t_1^k)$ where $\text{decode}(t_1^k) \in \text{prefix}(x_1^n)$ as follows:

$$P(x_1^n, t_1^k) = \sum_{\substack{\vec{t}' \in \text{cover}(x_1^n) \\ t_1^k = \vec{t}'_{[1:k]}}} P(\vec{t}'), \quad (3)$$

i.e., to compute $P(x_1^n, t_1^k)$, we limit the set of cover encodings to those that starts with t_1^k .

Proof. See Appendix A.3.

Finally, to apply Lemma 1, we need to search for all $\vec{t} \in \text{cover}(x_1^n)$, which can be time consuming with naive search. For the tokenizers under consideration, i.e. BPE and MPE, there exists an efficient algorithm by using the properties of invalid encodings (Definition 3). We explain this algorithm in Section 4.1.1.

4.1.1 COVER ENCODING SEARCH ALGORITHM

We present the cover search process in Algorithm 1, which is illustrated in Figure 4 (right). Note that the algorithm also returns $P(\vec{t})$ for $\vec{t} \in \text{cover}(x_1^n)$ which we will use for the sampling later on. The idea is as follows: instead of searching for cover encodings from left to right, which can be computationally expensive, we search for valid encodings in reverse order, starting from the right. Suppose the last token t_k , of a cover encoding t_1^k is known and it has suffix x_{i+1}^n , then according to Proposition 1, we must have: $t_1^{k-1} = \text{encode}(x_1^i)$, else t_1^k will be invalid.

As a result, searching from the reverse order, for any suffix x_{i+1}^n , we can find all tokens that start with x_{i+1}^n , tokenize x_1^i and check if their combination is valid or not. The number of model runs is at most $n\ell$, where ℓ is length of the longest token in \mathcal{V} , in order to compute $P(\vec{t})$. In practice, the actual number of inference runs is much lower since $\text{encode}(x_1^i)$ of the current iterations often contains encodings of the later iterations. Finally, while we can obtain $P(x_{n+1}|x_1^n)$ through factorization using this algorithm, it is not practical for sampling purpose as we need to repeat the process for all $x_{n+1} \in \mathcal{A}$. We next show an efficient alternative in Section 4.2.

Algorithm 1 (Cover Encodings Search). Compute $P(x_1^n)$ and $P(\vec{t})$ for each $\vec{t} \in \text{cover}(x_1^n)$.

```

1: procedure EXTRACT_COVER( $x_1^N$ )
2:   cover_dict = {} # Dictionary  $\{\vec{t} : P(\vec{t})\}$ 
3:   for  $i = n - 1, \dots, 0$  do
4:     # Find all tokens covering  $x_{i+1}^n$  and tokenize the remaining  $x_1^i$ 
5:      $\mathcal{B} = \{t \in \mathcal{V} \mid x_{i+1}^n \in \text{prefix}(\text{decode}(t))\}$ 
6:      $t_1^{k-1} = \text{encode}(x_1^i)$ 
7:     # Compute  $P(t_1^k)$  where  $t_1^k = t_1, \dots, t_{k-1}, t$  for all  $t \in \mathcal{V}$ 
8:      $P(t_1^k) = P(t_1^{k-1}) \times P(t_{k+1} = t \mid t_1^{k-1})$  # Broadcast Multiplication for all  $t$ 
9:     # Remove invalid encodings.
10:    for  $t \in \mathcal{B}$  do
11:       $\vec{t} = \text{concat}(t_1^{k-1}, t)$ 
12:      cover_dict[ $\vec{t}$ ] =  $P(\vec{t})$  if is_valid( $\vec{t}$ )
13:    end for
14:  end for
15:  #  $\text{cover}(x_1^n) = \text{cover\_dict.keys}()$ 
16:   $P(x_1^n) = \sum_{\vec{t} \in \text{cover\_dict}} P(\vec{t})$  # from the BTR Lemma ( Lemma 1).
17:  return  $P(x_1^n)$ , cover_dict
18: end procedure

```

4.2 EFFICIENT NEXT-BYTE SAMPLING ALGORITHM FOR $P(x_{n+1} \mid x_1^n)$

To efficiently compute $P(x_{n+1} \mid x_1^n)$ for any $x_{n+1} = a \in \mathcal{A}$, we note that $\text{cover}(x_1^{n+1})$ contains:

- $C_{n+1}(a)$: encodings \vec{t} from the previous $\text{cover}(x_1^n)$ whose $(n+1)^{\text{th}}$ bytes is a . Formally, we have: $C_{n+1}(a) = \{\vec{t} \in \text{cover}(x_1^n) \mid \text{decode}(\vec{t})_{n+1} = a\}$.
- $\bar{C}_{n+1}(a)$: encodings \vec{t} whose last token starts with a at the $(n+1)$ location. Formally, we have: $\bar{C}_{n+1}(a) = \{t_1^{k+1} \mid t_1^k = \text{encode}(x_1^n), \text{decode}(t_{k+1})_1 = a\}$.

Since $C_{n+1}(a) \cap \bar{C}_{n+1}(a) = \emptyset$, then:

$$P(x_1^n, x_{n+1} = a) = \sum_{C_{n+1}(a)} P(\vec{t}) + \sum_{\bar{C}_{n+1}(a)} P(\vec{t}), \quad (4)$$

With this formulation, we find $\text{cover}(x_1^{n+1})$ following the process in Figure 5 (also see Algorithm 3 in Appendix A.8). Specifically, to find $C_{n+1}(a)$ and $\bar{C}_{n+1}(a)$ for every $a \in \mathcal{A}$, we:

1. Obtain $\text{cover}(x_1^n)$ using Algorithm 1 or from Step 4 of the previous sample.
2. Find $C_{n+1}(a)$ by checking the $(n+1)^{\text{th}}$ byte of each $\vec{t} \in \text{cover}(x_1^n)$. We accumulate them for each a respectively.
3. Find $\bar{C}_{n+1}(a)$ by querying the conditional distribution over all tokens $P(t_{k+1} \mid t_1^k)$. Note that $P(t_1^k)$ was already computed in $\text{cover}(x_1^n)$. The encoding accept/reject step is optional.
4. Obtain $\text{cover}(x_1^{n+1})$ for all $x_{n+1} = a \in \mathcal{A}$.
5. Sample x_{n+1} from all computed $P(x_1^{n+1})$ (normalizing by $P(x_1^n)$).

As a result, we only need to run Algorithm 1 at the beginning of the sampling process. For Step 3, the mapping of what tokens start with what bytes can be pre-computed and the sum over tokens can be parallelized via matrix multiplication. Also, one can avoid storing a large number of encodings at Step 4 by sampling the next byte immediately after Step 3, following Equation (4), and only create the set of the sampled value x_{n+1} , i.e. $\bar{C}_{n+1}(x_{n+1})$.

Remark 2. Computing $P(x_1^n)$ requires accessing to $P(t_1)$ but models such as the Yi series (Young et al., 2024) do not provide $P(t_1)$. Nevertheless, it is possible to compute $P(x_{n+1} \mid x_1^n)$ by leveraging the pre-tokenization pattern such as white spaces or punctuation. Details in Appendix A.1.

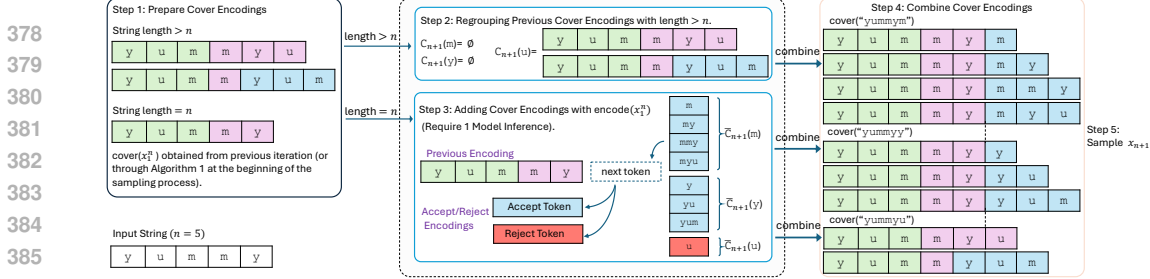


Figure 5: Illustration of the sampling process for x_{n+1} from tokenized LM $P(t_{k+1}|t_1^k)$, with example following Figure 4. We do not include $P(\bar{t})$ for simplicity. Details in Section 4.2.

5 RELATED WORK

Algorithms for Tokenization Bias. Tokenization bias has been empirically observed when model produces unusual generations when prompted with string ends with trailing whitespace (Gao et al., 2023) or mid-word (Dagan et al., 2024). Token healing (Dagan et al., 2024; guidance ai, 2023) mitigates this issue by searching for tokens prefixed with the incomplete word. This method, however, fails to consider all matching possibilities. In the “yummy” example in Figure 4, it can only recover two encodings “yum|my” and “yum|myu” (tokens separated by “|”), as “my” is a prefix string of tokens “my” and “myu”, missing “yum|yum” (also see Appendix D). Other proposed solution is using specific prompting strategies (Bavarian et al. (2022), also see PSM Mode in Section 6.1), requiring additional training and specific prompt structure. In contrast, we tackle the underlying issue by identifying the probabilistic root cause, i.e. the token-byte domain gap, and introduce a conversion technique to recover the unbiased byte-level distribution without requiring retraining. Finally, Pimentel & Meister (2024) address a different but related problem of computing next word probability, sharing some similar analysis. Unlike our work, their approach is limited to whitespace-separated tokenizers and does not support autoregressive byte sampling.

Language Model Ensembles To the best of our knowledge, our work is the first to (i) compute next token probabilities in a universal space for both input and output domains while (ii) guaranteeing that the statistical properties of all member models are preserved (see Section 4), and (iii) without the need for additional training, data or model modifications. Several works also attempted to combine multiple LMs. Wan et al. (2024) introduce a model distillation technique by combining predictions from various LMs to fine-tune a primary model, which does not tackle the issue of vocabulary discrepancies. Jiang et al. (2023b) use ranking approach and evaluating outputs at the paragraph level and comparing them pairwise. However, their approach requires training a scoring function, making it sensitive to the distribution of training data and model choice. Huang et al. (2024) maps the token probabilities of member models to a universal space, which relies on token embedding’s similarity and involves solving an optimization task. Gu et al. (2024) also investigate character-level ensembling, but does not provide expressions for $P(x_1^n)$ or $P(x_{n+1}|x_1^n)$ and overlooks the issue of invalid encodings. Since their method condition on tokens without addressing the bias, it is susceptible to invalid encoding states and division-by-zero errors, particularly with optimal sources.

6 EXPERIMENTS

6.1 CODE COMPLETION

Code completion with LLMs is well-suited for our byte-level predictions because the model is frequently prompted with incomplete code snippets. Here, we briefly introduce the setting and show that the byte-level predictions significantly improve upon the standard performance.

Fill-in-the-middle (FIM) code completion. Code completion is the process of taking source code as input along with a point in the middle to generate the completion, e.g., the point the user’s cursor is at. So, generating new code in the middle does not fit into the standard autoregressive generation provided by pre-training models, nor does it fit into standard system-user-assistant conversation prompt templates. The solution has been to introduce a fill-in-the-middle (FIM) prompt template that turns the middle generation back into a standard prompt that can be completed by an autoregressive model (Bavarian et al., 2022). These FIM prompt templates introduce new tokens or control sequences and cannot be used with a model that is not aware of them, so code models are then trained (or fine-tuned) on a dataset of code formatted into these FIM prompt templates.

Predictions	PSM		SPM	
	Greedy	@10	Greedy	@10
Token-level	64.9	84.0	45.0	66.5
+ healing			62.7	83.8
+ alignment			63.0	82.9
Byte-level	65.7	84.1	63.9	84.3

@10 here is the max over the temperature sweep on the right

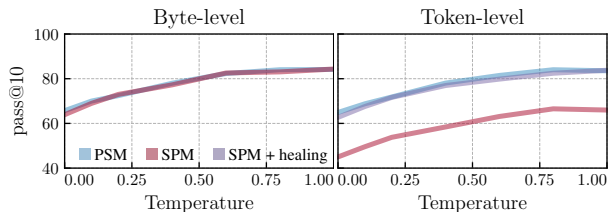


Figure 6: Pass rates for the HumanEval Random Span benchmark from Bavarian et al. (2022) with CodeLlama-7b for infilling Python. Across all settings, the byte-level predictions yield better completions. We evaluate the two standard infilling prompt templates of Prefix-Suffix-Middle (PSM) and Suffix-Prefix-Middle (SPM), and as baselines use token healing (Dagan et al., 2024) and alignment (Athiwaratkun et al., 2024). The SPM template forces the model to make predictions from the middle of a token, which our byte-level predictions successfully handle.

Prompt templates for FIM. Given a {prefix} and {suffix} along with the control tokens <PRE>, <MID>, and <SUF>, there are two main prompt formats for querying a code model to generate the middle portion: the Prefix-Suffix-Middle (PSM) format "<PRE> {prefix} <SUF>{suffix} <MID>", and Suffix-Prefix-Middle (SPM) format is "<PRE> <SUF>{suffix} <MID> {prefix}".

Upsides and downsides of PSM and SPM. The default and most widely-used mode is PSM (Bavarian et al., 2022; Roziere et al., 2023). We speculate this is the default mode because there are no tokenization issues in it: the incomplete prefix is clearly separated from the middle portion to generate by the control tokens. While the PSM format solves tokenization issues with this separation, the downside is that it creates an unnatural separation between the prefix and middle generation. SPM mode overcomes this by prompting the model to generate immediately after the prefix, without any separating tokens. This contiguity is desirable as it would leverage more knowledge from the pre-training task, but now creates a tokenization issue when the prefix stops in the middle of a token. A standard heuristic to overcoming this in SPM mode is called *token healing*, e.g., as described in Dagan et al. (2024), but it does not correct every tokenization issue here. Another fix is token-alignment (Athiwaratkun et al., 2024) but the scheme is biased and suboptimal (see Appendix E). These tokenization issues make the PSM template outperform the SPM template in every previous results for code infilling.

Our results. We experimented with the standard random-span infilling benchmark from (Bavarian et al., 2022). Figure 6 shows that our byte-level predictions in SPM mode attain superior performance when using 10 samples, using CodeLlama-7b. This corroborates our hypothesis that the contiguity between the prompted prefix and generated middle in SPM mode is more natural and consistent with the pre-training objective of the model. Another surprising result is that the byte-level greedy generations outperform the token-level greedy generations.

Ablation This is surprising because each token typically spans over multiple bytes, hence for greedy generation the token model should have a slight advantage. We wanted to further investigate this finding and hence performed beam search with beam width 2 and 4, which led to consistent improvement of up to 2.9% and best performance at 67.7. The complete ablation is located in Appendix C.

6.2 MODEL ENSEMBLES

Ensemble methods rely on two principles; model prediction averaging (aggregation) and training each member of a model ensemble on a subset of all available data (bootstrapping). Ensemble methods are a popular choice because aggregation reduces the variance of the expected empirical test error, and bootstrapping reduces model bias. As a result, bootstrap aggregation leads to model ensembles that are generally more accurate and robust than any individual member model (Hastie et al., 2009). The recent surge of open-weights LMs, each presumably trained on different subsets of available text, makes these LLMs ideal candidates for bootstrap aggregation.

Our method. Unfortunately, vocabulary discrepancies between LMs prevent direct aggregation, as models map to different token spaces. Our method solves this by enabling exact next-byte prediction, allowing any LM to map into the same space, so byte probabilities can be aggregated without restrictions on the aggregation function and preserving the statistical properties of the member models. In this work, we choose simple averaging. We leave more complex methods for future work.

	MMLU		PIQA		NQ		TriviaQA		GSM8K	
Model	Token	Byte	Token	Byte	Token	Byte	Token	Byte	Token	Byte
Llama2-7B	45.4	45.7	78.1	78.2	25.0	23.4	58.4	58.1	15.1	12.5
Yi-1.5-6B	63.4	63.4	78.5	78.5	22.8	22.7	53.7	53.4	61.3	61.5
Mistral-7B-v0.3	62.1	62.1	80.1	80.3	28.5	28.8	63.6	63.5	39.0	39.0
Voting (top-2)		62.1		80.1						
Top-2 ensemble (Our)		65.4		80.7		30.0		64.2		55.8

Table 1: We evaluate the token and equivalent byte-level model performance of various open source LMs. We further show the byte-ensemble performance of the top-2 performing models. For all benchmarks but GSM8K, byte-level ensembles outperform single models and voting.

Benchmarks and setup. We compare next-token, next-byte, voting and byte-ensembles against one another on multiple knowledge, reasoning, and coding benchmarks. We chose our benchmarks due to their prevalence in testing general LM ability. Due to computational constraints, we test on 7B models primarily. Note that multiple choice tasks require likelihood evaluation (MMLU, PIQA) while other tasks require mid to long generations. Finally, voting is not trivially extended to reasoning tasks without training an evaluator network.

Our results. The results of this experiment are in Table 1 and 2. Byte and token predictions are often on par with one another. Ensembling the top-2 performing models seems consistently lead to performance boost except when member model performance is too divergent, as in the case of GSM8K dataset where Yi-1.5-6B outperforms Mistral-7B-v0.3, the second best model, by a margin of 20%. For coding tasks, the ensemble of Yi-Coder-1.5B and CodeLlama2-13b improves up to 3.7% on Human Eval dataset. Overall, these results show the benefits of ensemble as an exciting direction for LMs collaboration.

	Human Eval @1		MBPP@1	
Model	Token	Byte	Token	Byte
CodeLlama2-7b	32.3	28.7	40.6	42.4
CodeLlama2-13b	35.8	33.5	47.6	47.4
Yi-Coder-1.5B	38.4	36.5	52.8	53.6
Top-2 Ensemble		42.1		53.6

Table 2: We evaluate the token and equivalent byte-level model performance of open-weight code LMs. We show the byte-ensemble performance of the top-2 performing models. Ensemble Model achieves best result on Human Eval benchmark while drawing Yi-Coder-1.5B on MBPP.

7 CONCLUSION

Conclusion and limitations. This work shows that tokenized LMs have different predictive distributions than their statistically equivalent byte-level counterpart, i.e. tokenization bias. We introduced an $O(1)$ next-byte prediction algorithm to mitigate this bias at inference time and showed its empirical relevance for FIM benchmarks and model ensemble tasks. Yet, our method introduces notable memory consumption in its current implementation, and incurs additional linear computational costs (one token = multiple bytes). At present, these factors may limit its practical application in resource-constrained environments. While our work provides new insights into the effects of tokenization, it can not explain or mitigate all related phenomena such as poor performance on arithmetic tasks.

Future work. While this work sheds some light on token- and byte-level LMs, several open questions remain. Notably, our theory does not provide insight into the employed greedy evaluation process, nor do we examine the cumulative impact of tokenization bias. Regarding the latter, our analysis is limited to single-token predictions, while real-world applications require generating hundreds of tokens. Building on our findings, future research can explore broader topics, such as bias-variance decomposition in LM ensembles, or interplays between bootstrapping and scaling laws. Apart from theoretical work, future development could explore model distillation, where larger models with larger vocabularies could be distilled into smaller models with specialized tokenization. It also enables model-independent prompt optimization, such as for universal adversarial attacks, and facilitates relative uncertainty estimation, allowing for comparisons of model uncertainty. Our work only scratched the surface of the possibility of model ensembles: For example, models trained on different languages may outperform a single model trained on all languages simultaneously, as individual models can achieve more optimal entropy bounds by utilizing distinct tokenizations tailored to their respective languages. This might also improve the representation of otherwise underrepresented languages in a training data corpus. Furthermore, our results also open up new possibilities for tackling mechanism design problems (Duetting et al., 2024) involving different language models, where the tokenization bias issue can potentially create unfair advantages for certain models.

REFERENCES

- 540
541
542 Ben Athiwaratkun, Shiqi Wang, Mingyue Shang, Yuchen Tian, Zijian Wang, Sujan Kumar Gou-
543 gondla, Sanjay Krishna Gouda, Rob Kwiatowski, Ramesh Nallapati, and Bing Xiang. Token
544 alignment via character matching for subword completion. *arXiv preprint arXiv:2403.08688*,
545 2024.
- 546 Mohammad Bavarian, Heewoo Jun, Nikolas Tezak, John Schulman, Christine McLeavey, Jerry
547 Tworek, and Mark Chen. Efficient training of language models to fill in the middle. *arXiv*
548 *preprint arXiv:2207.14255*, 2022.
- 549 Tom Brown, Benjamin Mann, Nick Ryder, Melanie Subbiah, Jared D Kaplan, Prafulla Dhariwal,
550 Arvind Neelakantan, Pranav Shyam, Girish Sastry, Amanda Askell, et al. Language models are
551 few-shot learners. *Advances in neural information processing systems*, 33:1877–1901, 2020.
552
- 553 Gautier Dagan, Gabriele Synnaeve, and Baptiste Rozière. Getting the most out of your tokenizer for
554 pre-training and domain adaptation. *arXiv preprint arXiv:2402.01035*, 2024.
- 555 Paul Duetting, Vahab Mirrokni, Renato Paes Leme, Haifeng Xu, and Song Zuo. Mechanism design
556 for large language models. In *Proceedings of the ACM on Web Conference 2024*, pp. 144–155,
557 2024.
558
- 559 L Gao, J Tow, B Abbasi, S Biderman, S Black, A DiPofi, C Foster, L Golding, J Hsu, A Le Noac’h,
560 et al. A framework for few-shot language model evaluation, 12 2023. URL <https://zenodo.org/records/10256836>, 7, 2023.
- 562 Omer Goldman, Avi Caciularu, Matan Eyal, Kris Cao, Idan Szpektor, and Reut Tsarfaty. Unpacking
563 tokenization: Evaluating text compression and its correlation with model performance. *arXiv*
564 *preprint arXiv:2403.06265*, 2024.
565
- 566 Kevin Gu, Eva Tuecke, Dmitriy Katz, Raya Horesh, David Alvarez-Melis, and Mikhail Yurochkin.
567 Chared: Character-wise ensemble decoding for large language models. *arXiv preprint*
568 *arXiv:2407.11009*, 2024.
- 569 guidance ai. Guidance ai, 2023. URL <https://github.com/guidance-ai/guidance>.
570 GitHub repository.
- 571 Trevor Hastie, Robert Tibshirani, Jerome H Friedman, and Jerome H Friedman. *The elements of*
572 *statistical learning: data mining, inference, and prediction*, volume 2. Springer, 2009.
573
- 574 Ari Holtzman, Jan Buys, Li Du, Maxwell Forbes, and Yejin Choi. The curious case of neural text
575 degeneration, 2020. URL <https://arxiv.org/abs/1904.09751>.
- 576 Yichong Huang, Xiaocheng Feng, Baohang Li, Yang Xiang, Hui Wang, Bing Qin, and Ting Liu.
577 Enabling ensemble learning for heterogeneous large language models with deep parallel collabo-
578 ration. *arXiv preprint arXiv:2404.12715*, 2024.
579
- 580 Albert Q. Jiang et al. Mistral 7b, 2023a. URL <https://arxiv.org/abs/2310.06825>.
- 581 Dongfu Jiang, Xiang Ren, and Bill Yuchen Lin. Llm-blender: Ensembling large language models
582 with pairwise ranking and generative fusion. *arXiv preprint arXiv:2306.02561*, 2023b.
583
- 584 Philipp Koehn and Rebecca Knowles. Six challenges for neural machine translation. In Thang
585 Luong, Alexandra Birch, Graham Neubig, and Andrew Finch (eds.), *Proceedings of the First*
586 *Workshop on Neural Machine Translation*, pp. 28–39, Vancouver, August 2017. Association for
587 Computational Linguistics. doi: 10.18653/v1/W17-3204. URL <https://aclanthology.org/W17-3204>.
588
- 589 Tomasz Limisiewicz, Terra Blevins, Hila Gonen, Orevaoghene Ahia, and Luke Zettlemoyer. Myte:
590 Morphology-driven byte encoding for better and fairer multilingual language modeling. *arXiv*
591 *preprint arXiv:2403.10691*, 2024.
592
- 593 Tiago Pimentel and Clara Meister. How to compute the probability of a word. *arXiv preprint*
arXiv:2406.14561, 2024.

- 594 Ivan Provilkov, Dmitrii Emelianenko, and Elena Voita. Bpe-dropout: Simple and effective subword
595 regularization. In *Proceedings of the 58th Annual Meeting of the Association for Computational*
596 *Linguistics*. Association for Computational Linguistics, 2020.
- 597 Nived Rajaraman, Jiantao Jiao, and Kannan Ramchandran. Toward a theory of tokenization in llms.
598 *arXiv preprint arXiv:2404.08335*, 2024.
- 600 Baptiste Roziere, Jonas Gehring, Fabian Gloeckle, Sten Sootla, Itai Gat, Xiaoqing Ellen Tan, Yossi
601 Adi, Jingyu Liu, Romain Sauvestre, Tal Remez, et al. Code llama: Open foundation models for
602 code. *arXiv preprint arXiv:2308.12950*, 2023.
- 603 Felix Stahlberg and Bill Byrne. On NMT search errors and model errors: Cat got your tongue?
604 In Kentaro Inui, Jing Jiang, Vincent Ng, and Xiaojun Wan (eds.), *Proceedings of the 2019 Con-*
605 *ference on Empirical Methods in Natural Language Processing and the 9th International Joint*
606 *Conference on Natural Language Processing (EMNLP-IJCNLP)*, pp. 3356–3362, Hong Kong,
607 China, November 2019. Association for Computational Linguistics. doi: 10.18653/v1/D19-1331.
608 URL <https://aclanthology.org/D19-1331>.
- 609 Hugo Touvron, Thibaut Lavril, Gautier Izacard, Xavier Martinet, Marie-Anne Lachaux, Timothée
610 Lacroix, Baptiste Rozière, Naman Goyal, Eric Hambro, Faisal Azhar, et al. Llama: Open and
611 efficient foundation language models. *arXiv preprint arXiv:2302.13971*, 2023.
- 612 Fanqi Wan, Xinting Huang, Deng Cai, Xiaojun Quan, Wei Bi, and Shuming Shi. Knowledge fusion
613 of large language models. *arXiv preprint arXiv:2401.10491*, 2024.
- 614 Alex Young, Bei Chen, Chao Li, Chengen Huang, Ge Zhang, Guanwei Zhang, Heng Li, Jiangcheng
615 Zhu, Jianqun Chen, Jing Chang, et al. Yi: Open foundation models by 01. ai. *arXiv preprint*
616 *arXiv:2403.04652*, 2024.
- 617 Lili Yu, Dániel Simig, Colin Flaherty, Armen Aghajanyan, Luke Zettlemoyer, and Mike Lewis.
618 Megabyte: Predicting million-byte sequences with multiscale transformers. *Advances in Neural*
619 *Information Processing Systems*, 36, 2024.
- 620 Vilém Zouhar, Clara Meister, Juan Gastaldi, Li Du, Mrinmaya Sachan, and Ryan Cotterell. Tok-
621 enization and the noiseless channel. In *Proceedings of the 61st Annual Meeting of the Association*
622 *for Computational Linguistics (Volume 1: Long Papers)*, pp. 5184–5207, 2023.
- 623
624
625
626
627
628
629
630
631
632
633
634
635
636
637
638
639
640
641
642
643
644
645
646
647

A APPENDIX

A.1 ESTIMATE $P(x_{n+1}|x_1^n)$ WHEN $P(t_1)$ IS NOT AVAILABLE

In practice, several models such as the Yi series do not provide $P(t_1)$ since it does not include the beginning of sequence token. As a result, we cannot compute $P(\vec{t})$. However, we can still compute $P(x_{n+1}|x_1^n)$ since their tokenization algorithm often force splitting words by using pre-tokenization pattern such as the whitespace. Let x_i be the last whitespace byte in x_1^n such that x_{i-1} is not a whitespace. Then we know that $t_1^k = \text{encode}(x_1^i)$ must be the prefix encoding of all cover encodings of x_1^n . This holds not only for x_1^n but also any string $s = \text{concat}(x_1^n, s')$ where s' is an arbitrary suffix.

As such, using the BTR Lemma 1, we have:

$$P(x_1^n) = \sum_{\vec{t} \in \text{cover}(x_1^n)} P(\vec{t}) = P(t_1^k) \times \sum_{\vec{t}' \in \text{cover}(x_{i+1}^n)} P(\vec{t}'|t_1^k) \quad (5)$$

and hence, with factorization:

$$P(x_{n+1}|x_1^n) = \left(\sum_{\vec{t}' \in \text{cover}(x_{i+1}^n)} P(\vec{t}'|t_1^k) \right) / \left(\sum_{\vec{t}' \in \text{cover}(x_{i+1}^n)} P(\vec{t}'|t_1^k) \right), \quad (6)$$

which shows that we do not need $P(t_1^k)$ to compute $P(x_{i+1}^n)$, since conditioning on them is sufficient. For autoregressive byte generation, we condition each probability term in Algorithm 3 with t_1^k .

A.2 PROOF OF LEMMA 1

Lemma 1. (Byte-Token Representation Lemma) For a consistent tokenizer and a corresponding language model $P(t_{k+1}|t_1^k)$, given a prefix x_1^n , we have the followings:

1. For any distinct $\vec{t}, \vec{t}' \in \text{cover}(x_1^n)$, then $\mathcal{X}(\vec{t}) \cap \mathcal{X}(\vec{t}') = \emptyset$.
2. $\mathcal{X}(x_1^n) = \bigcup_{\vec{t} \in \text{cover}(x_1^n)} \mathcal{X}(\vec{t})$.

As a result, $P(x_1^n)$ can be expressed as the marginal probability of all covering tokens of x_1^n

$$P(x_1^n) = \sum_{\vec{t} \in \text{cover}(x_1^n)} P(\vec{t}). \quad (7)$$

Proof. We prove each point as follows:

1. Proof by contradiction, let $t_1^i, t_1^j \in \text{cover}(x_1^n)$ and $t_1^i \neq t_1^j$. Suppose that there exists a sequence \mathbf{x} where $t_1^i = \text{encode}(\mathbf{x})_1^i$ and $t_1^j = \text{encode}(\mathbf{x})_1^j$. Without the loss of generalization, suppose $i < j$, then $t_1^i = t_1^j$ since our tokenizer is deterministic. Hence, t_1^j cannot be a cover encoding of x_1^n .
2. This follows the definition of cover encodings.

Since each $\mathcal{X}(\vec{t})$ is pair-wise disjoint, we arrive at the final equation. \square

A.3 PROOF OF COROLLARY 1

Corollary 1. We can express $P(x_1^n, t_1^k)$ where $\text{decode}(t_1^k) \in \text{prefix}(x_1^n)$ as follows:

$$P(x_1^n, t_1^k) = \sum_{\substack{\vec{t} \in \text{cover}(x_1^n) \\ t_1^k = \vec{t}_{[1:k]}}} P(\vec{t}). \quad (8)$$

Algorithm 2 Byte Pair Encoding Algorithm.

```

702 1: procedure ENCODE_BPE( $x_1^N, \mathcal{V}$ )
703 2:   # Set initial encodings:
704 3:   c_tokens =  $x_1^N$ 
705 4:   # Iterate over merging order in  $\mathcal{V}$ , the first  $|\mathcal{A}|$  entries correspond the the alphabet (no merge happens):
706 5:   for  $i = |\mathcal{A}| + 1, \dots, |\mathcal{V}|$  do
707 6:     c_tokens  $\leftarrow$  find_merge(c_tokens,  $\mathcal{V}[i]$ )
708 7:   end for
709 8:   return c_tokens
710 9: end procedure
711 10:
712 11: procedure find_merge(c_tokens,  $v$ )
713 12:   # Left and right tokens for merging
714 13:    $t_{\text{left}}, t_{\text{right}}, t_{\text{new}} = v[1], v[2], v[3]$ 
715 14:   old_tokens = c_tokens
716 15:   new_tokens = []
717 16:   # Find and merge tokens from left to right
718 17:    $j = 1$ 
719 18:   while  $j < |\text{old\_tokens}|$  do
720 19:     if old_tokens[ $i, i + 1$ ] =  $t_{\text{left}}, t_{\text{right}}$  then
721 20:       new_tokens.append( $t_{\text{new}}$ )
722 21:        $j = j + 2$ 
723 22:     else
724 23:       new_tokens.append(old_tokens[ $i$ ])
725 24:        $j = j + 1$ 
726 25:     end if
727 26:   end while
728 27:   return new_tokens
729 28: end procedure

```

Proof. The proof follows the one for the BTR Lemma 1, where we only consider the cover encodings that start with t_1^k . \square

A.4 PROOF OF PROPOSITION 1

For completeness, we first show the BPE encoding algorithm in Algorithm 2. For the MPE algorithm, the rule is greedily looking for the longest token that matches the prefix of the given text.

Proposition 1. $\mathcal{X}(t_1^k) = \emptyset$ if and only if t_1^k is invalid.

Proof. For the case of BPE, we prove each direction as follows.

- If $\mathcal{X}(t_1^k) = \emptyset$ then t_1^k is invalid: Since $\mathcal{X}(t_1^k) = \emptyset$, we know that there exist no sequence \mathbf{x} such that $\text{encode}(\mathbf{x})_1^k = t_1^k$. This means there is also no string s that satisfy $\text{encode}(s)_1^k = t_1^k$. As such, for $s = \text{decode}(t_1^k)$, we do not have $\text{encode}(\text{decode}(t_1^k)) = t_1^k$, which proves the result.
- If t_1^k is invalid then $\mathcal{X}(t_1^k) = \emptyset$: Let $x_1^n = \text{decode}(t_1^k)$, it is sufficient to consider two string s_1 and s_2 that both have prefix x_1^n . Furthermore, we assume the first i tokens of s_1 covers exactly x_1^n , i.e. $x_1^n = \text{decode}(t_1^i)$ and similarly, the first j tokens of s_2 covers exactly x_1^n , i.e. $x_1^n = \text{decode}(t_1^j)$. Then:
 1. Proving invalid t_1^k leads to $\mathcal{X}(t_1^k) = \emptyset$ is equivalently to proving $t_1^i = t_1^j$ for any s_1, s_2 .
 2. Re-running the BPE algorithm for s_1 and s_2 in parallel, we know that there will be no merge between any suffix of x_1^n and the rest of strings, i.e. $s_1 \setminus x_1^n$ and $s_2 \setminus x_1^n$ due to the condition above (See Algorithm 2, line 6).
 3. Furthermore, for s_1 , any time a merge happens within x_1^n then the same merge must also happen within x_1^n for s_2 and vice versa.

As the result, we have $t_1^i = t_1^j$ and they must be equal to $\text{encode}(x_1^n)$.

For the case of MPE, the proof is similar:

- If $\mathcal{X}(t_1^k) = \emptyset$ then t_1^k is invalid: Since $\mathcal{X}(t_1^k) = \emptyset$, similar to the case of BPE, we know that there exist no string s such that $\text{encode}(s)_1^k = t_1^k$. As such, for $s = \text{decode}(t_1^k)$, we do not have $\text{encode}(\text{decode}(t_1^k)) = t_1^k$, which proves the result.
- If t_1^k is invalid then $\mathcal{X}(t_1^k) = \emptyset$: Let $x_1^n = \text{decode}(t_1^k)$, we consider two string s_1 and s_2 that both have prefix x_1^n . Furthermore, we assume the first i tokens of s_1 covers exactly x_1^n , i.e. $x_1^n = \text{decode}(t_1^i)$ and similarly, the first j tokens of s_2 covers exactly x_1^n , i.e. $x_1^n = \text{decode}(t_1^j)$. Since the MPE tokenizer will greedily looking for the longest token, hence one of the the encodings must not follow MPE encoding rule (contradiction).

This concludes the proof. \square

A.5 TOKENIZATION BIAS UNDER STOCHASTIC TOKENIZERS

Another class of tokenizers is non-deterministic, such as BPE Dropout (Provilkov et al., 2020), to address model’s weakness against text fragmentation by randomly omitting tokens before text processing, theoretically training the model in multiple vocabularies. Although intended to enhance robustness, our analysis suggests that tokenization bias still exists despite less obvious. It is partially mitigated, nevertheless, since the model needs to minimize loss across varied vocabulary sets. The BTR lemma (Lemma 1) holds, requiring consideration of all valid encodings under this variability. In practice, given the substantial size of the vocabulary, BPE-dropout is expected to be robust to tokenization bias, i.e. assigning non-zero probabilities to invalid encodings. Yet, it is not commonly employed in training large-scale LLMs because the randomized tokenization introduces a computational bottleneck, which slows down the training process. Also, it may require greater model capacity to handle the increased complexity.

We demonstrate the tokenization bias in BPE-droupt in the following experiment. Here, we use the 1st order Markov chain example as in Figure 2 where $(\alpha, \beta) = (0.4, 0.3)$. We train a LLM with BPE dropout where a sequence can be tokenized either with the vocabulary $\mathcal{V}_1 = \{\text{“A”}, \text{“B”}, \text{“AA”}\}$ or $\mathcal{V}_2 = \{\text{“A”}, \text{“B”}\}$ with equal probability. Consider the following input tokens (separated by |) and their next-token probabilities:

- “|B|A|” and next token probabilities $\{\text{“A”} : 0.43, \text{“B”} : 0.57, \text{“AA”} : 10^{-5}\}$: tokenization bias happens according to Definition 2 but the probability does not go to 0.0 as the cross entropy loss is distributed between the two vocabularies.
- “|B|A|A|” and next token probabilities $\{\text{“A”} : 0.59, \text{“B”} : 0.41, \text{“AA”} : 10^{-5}\}$: which approximately equal to the original byte-level probabilities since the LLM detects that the only possible vocabulary that produces these tokens is $\mathcal{V}_2 = \{\text{“A”}, \text{“B”}\}$.
- “|B|AA|A|” and next token probabilities $\{\text{“A”} : 10^{-4}, \text{“B”} : 0.99, \text{“AA”} : 10^{-5}\}$: tokenization bias occurs, i.e. the LM only outputs token “B”. Since “AA” only occurs in the vocabulary $\mathcal{V}_1 = \{\text{“A”}, \text{“B”}, \text{“AA”}\}$, the LLM detects the tokenization pattern and infer that the sequence must be tokenized with this vocabulary.

Finally, for the first case “BA”, we can recover the exact probability by using the BTR lemma. In this case, its cover encoding and associated probabilities are $t_1 = |B|A|, t_2 = |B|AA|$ and $P(t_1) = 0.104$ and $P(t_2) = 0.0415$. For the string “BAA”, the first cover encoding is t_2 , which is already computed and the other one is $t_3 = |B|A|A|$ and $P(t_3) = 0.0443$. Using factorization, we obtain $\alpha = 0.405$, which is approximately equal the the original value of 0.4.

A.6 ON PREDICTIVE DISTRIBUTION OF LANGUAGE MODELS

In practice, LMs often do not strictly follow Proposition 1 due to softmax activations. In this section, we show that given any tokenized LM, we can force its output probabilities to obey Proposition 1, without any loss in terms of perplexity score on the token domain. In other words, we can turn a

810 tokenized language model that does not follow Proposition 1 to the one that does while guaranteeing
 811 that the new model will always result in a lower token-level perplexity score.

812 We first introduce Proposition 2. In this proposition, we are given a target discrete probability distri-
 813 bution p where we know some of the values will not happen, says Φ^* . Assume that we have another
 814 distribution q that approximates p , then we can produce another distribution q^* that is closer to p in
 815 terms of KL divergence by setting corresponding probabilities of q in Φ^* to 0.0 and renormalize it.

816 **Proposition 2.** *Given a discrete distribution $p = \{p_1, p_2, \dots, p_m\}$ and $q = \{q_1, q_2, \dots, q_m\}$ with
 817 $q_i > 0.0$ for all i . Let $\Phi = \{i \in \mathbb{Z} | p_i = 0.0\}$ and $\Phi^* \subseteq \Phi$, we define $q^* = \{q_1^*, q_2^*, \dots, q_m^*\}$ where
 818 $q_i^* = 0.0$ for $i \in \Phi^*$, and $q_j^* = q_j / (\sum_{l \notin \Phi^*} q_l)$. Then we have:*

$$819 \quad D_{\text{KL}}(p || q^*) \leq D_{\text{KL}}(p || q), \quad (9)$$

820 which implies that q^* is closer to p than q . We refer to the process of producing q^* as truncate-
 821 renormalization (TR).

822 *Proof.* Let $Z = (\sum_{l \notin \Phi^*} q_l)$ is the normalizing factor in q^* . Note that $Z \leq 1$ and as such $\log(Z) \leq 0$.
 823 Then:

$$824 \quad D_{\text{KL}}(p || q^*) = \sum_i p_i \log \left(\frac{p_i}{q_i^*} \right) \quad (10)$$

$$825 \quad = \sum_{i \notin \Phi^*} p_i \log \left(\frac{p_i}{q_i^*} \right) \quad , \text{ use } 0 \log 0 = 0.0 \quad (11)$$

$$826 \quad = \sum_{i \notin \Phi^*} p_i \log \left(\frac{p_i}{q_i / Z} \right) \quad (12)$$

$$827 \quad = \left[\sum_{i \notin \Phi^*} p_i \log \left(\frac{p_i}{q_i} \right) \right] + \log(Z) \quad (13)$$

$$828 \quad \leq \sum_{i \notin \Phi^*} p_i \log \left(\frac{p_i}{q_i} \right) = D_{\text{KL}}(p || q), \quad (14)$$

829 which completes the proof. □

830 Applying to our scenario, for any autoregressive LM $P_1(t_{k+1} | t_1^k)$ that does not follow Proposition 1
 831 (due to the softmax activations), we can perform the TR process (since we know which encoding is
 832 invalid) to obtain a new LM $P_2(t_{k+1} | t_1^k)$, which is guaranteed to better approximate the ground-truth
 833 model $P(t_{k+1} | t_1^k)$. Thus, we are guaranteed that the token-level perplexity score of $P_2(t_{k+1} | t_1^k)$
 834 is always lower than or equal to $P_1(t_{k+1} | t_1^k)$. Finally, in practice, we observe that the conditional
 835 $P_1(t_{k+1} | t_1^k)$ for invalid t_1^{k+1} is significantly smaller than the valid tokens.

836 A.7 THE MARKOV CHAIN EXAMPLE

837 We provide a detail computation of the Markov chain example in the main paper. Recall that in the
 838 original chain (in the character domain), we have the following:

$$839 \quad P(x_2 = \text{"A"} | x_1 = \text{"A"}) = 1 - \alpha \quad (15)$$

$$840 \quad P(x_2 = \text{"B"} | x_1 = \text{"A"}) = \alpha \quad (16)$$

$$841 \quad P(x_2 = \text{"A"} | x_1 = \text{"B"}) = \beta \quad (17)$$

$$842 \quad P(x_2 = \text{"B"} | x_1 = \text{"B"}) = 1 - \beta \quad (18)$$

843 We also assume the initial probability $\pi = \{\gamma, 1 - \gamma\}$ for "A" and "B" respectively. In the token
 844 domain, let first compute $P(t_2 = \text{"A"} | t_1 = \text{"AA"})$ where we have:

$$845 \quad P(t_2 = \text{"A"} | t_1 = \text{"AA"}) = P(x_3^6 = \text{"ABA"} | x_1^2 = \text{"AA"}) + P(x_3^6 = \text{"ABB"} | x_1^2 = \text{"AA"}) \quad (19)$$

$$846 \quad = P(x_3^5 = \text{"AB"} | x_1^2 = \text{"AA"}) \quad (20)$$

$$847 \quad = \alpha(1 - \alpha), \quad (21)$$

where in the first equality, we do not include the case $x_3^6 = \text{"AAA"}$ and $x_3^6 = \text{"AAB"}$ since $\text{encode}(\text{"AAA"})_1 = \text{"AA"}$ and $\text{encode}(\text{"AAB"})_1 = \text{"AA"}$, which are not the token "A" that we are interested in. For other tokens when $t_1 = \text{"B"}$, the computation follows the same arguments.

Finally, for the case of $t_1 = \text{"A"}$, we note that it implies the second token must be "B" since any "A" after the first "A" must be tokenized into "AA" (invalid tokens). Hence, we have $P(t_2 = \text{"B"} | t_1 = \text{"A"}) = 1.0$. Finally, in this specific Markov chain, since order of the Markov chain in the character domain is 1, we do not need to consider the higher order of the Markov chain in the token domain.

Higher-Order Markov Chain Experiment Setup. We validate the estimated byte-level probabilities of the BTR Lemma (Lemma 1) using the Markov chain’s transition probabilities as ground truth. Specifically, we simulate the data generating process as a 3rd order Markov chain with two states $\mathcal{A} = \{\text{"A"}, \text{"B"}\}$, where we randomly construct the transition matrix and the vocabulary $\mathcal{V} = \{\text{"A"}, \text{"B"}, \text{"B\cdot A"}, \text{"BA\cdot A"}, \text{"B\cdot BAA"}, \text{"A\cdot A"}, \text{"BA\cdot BA"}, \text{"B\cdot B"}\}$. Here, the order within \mathcal{V} is the merging order for the BPE encoding process and the “.” separates the merging tokens. We then train a LM model using GPT-2 architecture with 6 hidden layers on the synthetically generated data. Since the model is agnostic to the Markov chain order, we average the probability from 100 runs on different context length while fixing the last 3 bytes.

A.8 NEXT-BYTE SAMPLING ALGORITHM

Algorithm 3 shows the next-byte algorithm in Section 4.2. Note that for $\tilde{C}_{n+1}(a)$, we do not need to iterate over every time since the mapping from tokens to their prefix byte can be precomputed (line 30-33).

B NOTEWORTHY IMPLEMENTATION CONSIDERATIONS

Theoretically, we do not have to predict into utf-8 byte space. We could predict into the largest set of tokens \mathcal{A} that is contained in the vocabularies of all members of our model ensemble: $\max_{\mathcal{A}} \|\mathcal{A}\|$ s.t. $A \subseteq \mathcal{V}_i$ for all i . This can have certain advantages, the primary one being that generation would be faster: for example imagine an average token has four bytes. Our method now needs to predict four times instead of one to generate the same expected amount of text. In this context, note that symbol based languages such as Chinese characters are often based on multiple bytes. Hence our method can be performance optimized by specializing the alphabet. Please note that our choice of alphabet does not change the statistical properties of the model, hence we would not expect accuracy differences due alphabet choice. However, the primary reason for us to choose the byte alphabet regardless was the ease of use for model ensemble: To run any experiment we need to map tokens probabilities to a **universal** alphabet, that is the easiest defining the alphabet as 255 bytes and the necessary control tokens.

C ABLATION: BEAM SEARCH

Each token is made of 6.6 byte on average. Thus, a tokenized model might have more foresight compared to a byte-level one when predicting one step at a time. Hence, even though, beam-search has not led to improvements in tokenized models (Holtzman et al., 2020; Stahlberg & Byrne, 2019; Koehn & Knowles, 2017), this might be different for byte-level models.

We repeat the FIM experiments with beam-width 1, 2 and 4, shown in Table 3. Consistently, we see an about 1% improvement for each prompting style and each beam-width increase. However, beam-search notably increases the memory footprint of any LLM because modern transformer based models need to store the KV-cache of each beam for efficient generation. Since the KV-cache makes about 2/3 of the overall memory consumption beam search is a memory intense operation.

Beam width	PSM	SPM
1	65.7	63.9
2	66.8	65.9
4	67.7	66.8

Table 3: Performance increases for the next-byte prediction on our FIM-task when beam search is applied.

Algorithm 3 Compute $P_{\mathcal{A}}(\cdot|x_1^n)$, which is a conditional distribution on x_1^n over all bytes $x \in \mathcal{A}$. $C_{n+1}(a)$ and $\bar{C}_{n+1}(a)$ also contain the encoding probability $P(\vec{t})$ for each encoding they contain.

```

918 1: procedure COMPUTE( $x_1^n$ , cover_dict( $x_1^n$ ) = None)
919 2:   if cover_dict( $x_1^n$ ) = None:
920 3:      $P(x_1^n)$ , cover_dict( $x_1^n$ ) = EXTRACT_COVER( $x_1^n$ )
921 4:     # Get the set  $C_{n+1}(a)$  (See Section 4.2) for all  $a \in \mathcal{A}$ 
922 5:     [ $C_{n+1}(a_1), \dots, C_{n+1}(a_{|\mathcal{A}|})$ ] = REGROUP_ENCODINGS(cover_dict( $x_1^n$ ))
923 6:     # Get the set  $\bar{C}_{n+1}(a)$  (See Section 4.2) for all  $a \in \mathcal{A}$ 
924 7:      $\vec{t}$  = encode( $x_1^n$ ); Query  $P(\vec{t})$  from cover_dict( $x_1^n$ ).
925 8:     [ $\bar{C}_{n+1}(a_1), \dots, \bar{C}_{n+1}(a_{|\mathcal{A}|})$ ] = ADD_NEW_ENCODINGS( $\vec{t}$ ,  $P(\vec{t})$ )
926 9:     # Merge cover dictionaries.
927 10:    for  $a \in \mathcal{A}$  do
928 11:       $x_{n+1} = a$ 
929 12:      cover_dict( $x_1^{n+1}$ ) =  $C_{n+1}(a) \cup \bar{C}_{n+1}(a)$ 
930 13:       $P(x_1^{n+1}) = \sum_{\vec{t} \in \text{cover\_dict}(x_1^{n+1})} P(\vec{t})$ 
931 14:    end for
932 15:    Obtain  $P_{\mathcal{A}}(\cdot|x_1^n)$  by renormalizing  $P(x_1^{n+1})$ .
933 16:    return  $P_{\mathcal{A}}(\cdot|x_1^n)$ , [cover_dict( $x_1^{n+1}$ ) for  $x_{n+1} = a \in \mathcal{A}$ ]
934 17: end procedure
935 18:
936 19: procedure REGROUP_ENCODINGS(cover_dict( $x_1^n$ ))
937 20:   for  $\vec{t}, P(\vec{t}) \in \text{cover\_dict}(x_1^n)$  do
938 21:     byte = decode( $\vec{t}$ )
939 22:      $C_{n+1}(\text{byte})[\vec{t}] = P(\vec{t})$ 
940 23:   end for
941 24:   return [ $C_{n+1}(a_1), \dots, C_{n+1}(a_{|\mathcal{A}|})$ ]
942 25: end procedure
943 26:
944 27: procedure ADD_NEW_ENCODINGS( $t_1^k$ ,  $P(t_1^k)$ )
945 28:   Compute  $P(t_{k+1} = t|t_1^k)$  for all  $t \in \mathcal{V}$  # Run 1 model inference for all  $t$ 
946 29:   Compute  $P(t_1^{k+1}) = P(t_{k+1} = t|t_1^k)P(t_1^k)$  for all  $t \in \mathcal{V}$  # Broadcasting for all  $t$ 
947 30:   for  $t \in \mathcal{V}$  do
948 31:     byte = decode( $t_1^{k+1}$ )
949 32:      $\bar{C}_{n+1}(\text{byte})[t_1^{k+1}] = P(t_1^{k+1})$ 
950 33:   end for
951 34:   return [ $\bar{C}_{n+1}(a_1), \dots, \bar{C}_{n+1}(a_{|\mathcal{A}|})$ ]
952 35: end procedure

```

D FIM CODE GENERATION EXAMPLES

Here, we show three examples from the random span FIM benchmark from Bavarian et al. (2022) that we evaluate on in Figure 6. Our greedy byte-level generations significantly improve upon the greedy token-level generations in the SPM (suffix-prefix-middle) mode with CodeLlama-7b because the prompt ends with the “prefix” portion of the code and the generation starts at a token boundary. Each figure visualizes an example from the benchmark with the prefix and suffix at the beginning and separated by <FILL-ME> indicating the portion for the LLM to generate. Then, we show the generations from the token and byte-level models in SPM mode along with token healing as a baseline. They illustrate exactly where tokenization issues arise when generating and show how the byte-level predictions correct them.

972 Listing 1: Code generation example with CodeLlama-7b. This one is interesting because of the
 973 typo in the variable “delimiter” in the dataset and the prefix ends with “delim”. The mis-
 974 spelled “delimiter” is tokenized as two tokens: “del imeter” while the correctly spelled
 975 “delimiter” is tokenized as a single token. This makes the 1) token-level prediction incorrectly
 976 generate “ter” as the continuation because “delimter” is tokenized as three tokens “del im
 977 ter”, which has a token boundary at the end of the prefix, 2) token-healed predictions incorrectly
 978 generate “iter” because at the token-level, “delimiter” is more likely, and 3) byte-level pre-
 979 dictions correctly generate “eter” because the probability at the byte-level correctly marginalizes
 980 out the byte-level probability despite the context and many possible tokenizations.

```

981 # RandomSpanInfilling/HumanEval/5/1
982 from typing import List
983
984 def intersperse(numbers: List[int], delimiter: int) -> List[int]:
985     """ Insert a number 'delimiter' between every two consecutive
986     ↪ elements of input list 'numbers'
987     >>> intersperse([], 4)
988     []
989     >>> intersperse([1, 2, 3], 4)
990     [1, 4, 2, 4, 3]
991     """
992     if not numbers:
993         return []
994
995     result = []
996
997     for n in numbers[:-1]:
998         result.append(n)
999         result.append(delim(FILL-ME)mbers[-1])
1000
1001     return result
1002
1003 token predictions (did not pass ✗):
1004 ter)
1005 result.append(nu
1006
1007 token predictions with token healing (did not pass ✗):
1008 iter )
1009 result.append(nu
1010
1011 byte predictions (passed ✓):
1012 eter)
1013 result.append(nu
  
```

1010 Listing 2: Code generation example with CodeLlama-7b. This one is interesting because of the
 1011 tokenization of “collatz” and the prefix starting with “colla”. “collatz” is tokenized as two
 1012 tokens “coll atz”. This makes the 1) token-level prediction incorrectly generate “zt” as the
 1013 continuation because “collazt” is tokenized as three tokens “col la zt”, which has a token
 1014 boundary at the end of the prefix, 2) token-healed predictions incorrectly generate “pse” because
 1015 at the token-level after backing up, “collapse” (a single token) is more likely, and 3) byte-level
 1016 predictions correctly generate “tz” because the probability at the byte-level correctly marginalizes
 1017 out the byte-level probability despite the context and many possible tokenizations.

```

1018 # RandomSpanInfilling/HumanEval/123/1
1019 def get_odd_collatz(n):
1020     """
1021     Given a positive integer n, return a sorted list that has the odd
1022     ↪ numbers in collatz sequence.
1023
1024     The Collatz conjecture is a conjecture in mathematics that concerns a
1025     ↪ sequence defined
1026     as follows: start with any positive integer n. Then each term is
1027     ↪ obtained from the
  
```

```

1026     previous term as follows: if the previous term is even, the next term
1027     ↪ is one half of
1028     the previous term. If the previous term is odd, the next term is 3
1029     ↪ times the previous
1030     term plus 1. The conjecture is that no matter what value of n, the
1031     ↪ sequence will always reach 1.
1032
1033     Note:
1034     1. Collatz(1) is [1].
1035     2. returned list sorted in increasing order.
1036
1037     For example:
1038     get_odd_collatz(5) returns [1, 5] # The collatz sequence for 5 is [5,
1039     ↪ 16, 8, 4, 2, 1], so the odd numbers are only 1, and 5.
1040     """
1041     if n%2==0:
1042         odd_collatz = []
1043     else:
1044         odd_colla (FILL-ME) 1
1045
1046         if n%2 == 1:
1047             odd_collatz.append(int(n))
1048
1049     return sorted(odd_collatz)
1050
1051 token predictions (did not pass ✗):
1052 zt = [n]
1053
1054     while n != 1:
1055         if n%2 == 0:
1056             n = n/2
1057         else:
1058             n = 3*n +
1059
1060 token predictions with token healing (did not pass ✗):
1061 pse = []
1062     odd_collatz = [n]
1063     while n != 1:
1064         if n%2 == 0:
1065             n = n/2
1066         else:
1067             n = 3*n +
1068
1069 byte predictions (passed ✓):
1070 tz = [n]
1071
1072     while n != 1:
1073         if n%2 == 0:
1074             n = n/2
1075         else:
1076             n = 3*n +

```

Listing 3: Code generation example with CodeLlama-7b. This one is interesting because of the tokenization of “palindrome” and the prefix starting with “palindr”. “palindrome” is tokenized as three tokens “pal ind rome”. This makes the 1) token-level prediction incorrectly generate “one” as the continuation because “palindrone” is tokenized as four tokens “pal ind r one”, which has a token boundary at the end of the prefix, 2) token-healed predictions incorrectly generate “eome” and results in the three-token chunk “pal indre ome” because the token healing did not successfully search backward enough, and 3) byte-level predictions correctly generate “ome” because the probability at the byte-level correctly marginalizes out the byte-level probability despite the context and many possible tokenizations.

```

1080
1081 # RandomSpanInfilling/HumanEval/107/8
1082 def even_odd_palindrome(n):
1083     """
1084     iven a positive integer n, return a tuple that has the number of even
1085     ↪ and odd
1086     integer palindromes that fall within the range(1, n), inclusive.
1087
1088     Example 1:
1089
1090     Input: 3
1091     Output: (1, 2)
1092     Explanation:
1093     Integer palindrome are 1, 2, 3. one of them is even, and two of
1094     ↪ them are odd.
1095
1096     Example 2:
1097
1098     Input: 12
1099     Output: (4, 6)
1100     Explanation:
1101     Integer palindrome are 1, 2, 3, 4, 5, 6, 7, 8, 9, 11. four of
1102     ↪ them are even, and 6 of them are odd.
1103
1104     Note:
1105     1. 1 <= n <= 10^3
1106     2. returned tuple has the number of even and odd integer
1107     ↪ palindromes respectively.
1108     """
1109     def is_palindr(FILL-ME) odd_palindrome_count = 0
1110
1111     for i in range(1, n+1):
1112         if i%2 == 1 and is_palindrome(i):
1113             odd_palindrome_count += 1
1114         elif i%2 == 0 and is_palindrome(i):
1115             even_palindrome_count += 1
1116     return (even_palindrome_count, odd_palindrome_count)
1117
1118 token predictions (did not pass ✗):
1119 one(n):
1120     return str(n) == str(n)[::-1]
1121
1122     def is_palindrome(n):
1123         return is_palindrone(n) and n >= 10
1124
1125     even_palindrome_count = 0
1126
1127 token predictions with token healing (did not pass ✗):
1128 eome(n):
1129     return str(n) == str(n)[::-1]
1130
1131     even_palindrome_count = 0
1132
1133 byte predictions (passed ✓):
1134 ome(n):
1135     return str(n) == str(n)[::-1]
1136
1137     even_palindrome_count = 0

```

1134 E ANALYSIS OF TOKEN ALIGNMENT
1135

1136 Recently, Athiwaratkun et al. (2024) also proposed a similar method to mitigate the tokenization
1137 bias issue. In this method, they start regenerating the last B tokens in the prompt by restricting
1138 the next-token to be either a prefix of the prompt’s remaining string or cover it, i.e. the remaining
1139 string is the prefix of the generated token. Although this appears to overlap with our Corollary 1, the
1140 sampling procedure is biased and can produce invalid encodings due to the greedy masking process.

1141 Consider the following example where we use the following vocabulary
1142 $\{<_>, <1>, <a>, <_a>, <_aa>\}$ with MPE tokenizer. For a prompt string “_a” which
1143 is tokenized as $<_a>$, token alignment will regenerate from the beginning and force the generated
1144 tokens to match the template “_a”. This is problematic when the first token generated is $<_>$.
1145 Given this token, tokenization bias occurs and the second token must not be $<a>$, since $<_a>$
1146 is a whole token. On the other hand, according to token alignment, the only possible next token
1147 after $<_>$ is $<a>$, but $<_><a>$ is an invalid encoding. The correct way to align is to by rejection
1148 sampling without greedy masking. We can use also our method by generating bytes until seeing a
1149 white space, then switch to token level generation. In this case, the prompt should exclude the last
1150 whitespace, and the first generated token must start with a whitespace.

1151
1152
1153
1154
1155
1156
1157
1158
1159
1160
1161
1162
1163
1164
1165
1166
1167
1168
1169
1170
1171
1172
1173
1174
1175
1176
1177
1178
1179
1180
1181
1182
1183
1184
1185
1186
1187